

Equation-of-Motion Approach to Dynamical Mean Field Theory

Jian-Xin Zhu, R. C. Albers, and J. M. Wills

Theoretical Division, Los Alamos National Laboratory, Los Alamos, New Mexico 87545

(Dated: March 23, 2022)

We propose using an equation-of-motion approach as an impurity solver for dynamical mean field theory. As an illustration of this technique, we consider a finite- U Hubbard model defined on the Bethe lattice with infinite connectivity at arbitrary filling. Depending on the filling, the spectra that is obtained exhibits a quasiparticle peak, and lower and upper Hubbard bands as typical features of strongly correlated materials. The results are also compared and in good agreement with exact diagonalization. We also find a different picture of the spectral weight transfer than the iterative perturbation theory.

PACS numbers: 71.30.+h, 71.10.Fd, 71.27.+a, 75.10.Lp

Theoretical understanding of strongly correlated electron systems has been a central and challenging problem in condensed matter physics. Dynamical mean field theory (DMFT) [1, 2, 3] has proven to be a very powerful theoretical tool that is not only tractable but also flexible enough to include material-specific details into the calculations. The essence of the DMFT is to map the lattice problem onto a single impurity problem plus a set of self-consistency conditions through which the characteristics of a specific lattice model enters. In particular, all models with only on-site Hubbard interaction can be mapped onto the single impurity Anderson model (SIAM) [4]. The problem is then to find a suitable solver for the SIAM. For the last few years, several numerical and analytical techniques to the SIAM have been explored. They include quantum Monte Carlo (QMC) [5, 6, 7], iterative perturbation theory (IPT) [8, 9, 10, 11], and exact diagonalization (ED) [12, 13]. Each method has its limitations. Except for some special models [14], QMC has difficulty in accessing very low temperatures, where statistical and finite time-step discretization errors become significant. Exact diagonalization, although exact, as the name implies, is limited by available computer time to a small number of orbitals, and hence it is difficult to obtain a smooth density of states. Iterative perturbation theory overcomes the drawbacks of these other two methods. However, in its original form, IPT is only valid at half filling. Away from half filling, it involves an ansatz and has instability problems.

The aim of this paper is to present an equation-of-motion (EOM) approach that can overcome the difficulties of QMC and ED while still maintaining the numerical efficiency and other advantages of IPT.

For concreteness, we demonstrate the method on the single-band Hubbard model for a Bethe lattice of infinite connectivity, $z \rightarrow \infty$. The Hamiltonian is

$$H = -\frac{t}{\sqrt{z}} \sum_{ij,\sigma} c_{i\sigma}^\dagger c_{j\sigma} + U \sum_i n_{i\uparrow} n_{i\downarrow}, \quad (1)$$

where t (fixed) is the hopping integral for electrons between z neighbors, n_i the occupation number on site i ,

and U is the on-site Hubbard interaction.

We study this model using the DMFT approach, which maps the model onto a self-consistent SIAM as given by the Hamiltonian:

$$H_{\text{SIAM}} = \sum_{k\sigma} \epsilon_{k\sigma} c_{k\sigma}^\dagger c_{k\sigma} + \sum_{k,\sigma} (V_{k\sigma} c_{k\sigma}^\dagger d_\sigma + V_{k\sigma}^* d_\sigma^\dagger c_{k\sigma}) + \sum_\sigma \epsilon_{d\sigma} d_\sigma^\dagger d_\sigma + U n_{d\uparrow} n_{d\downarrow}, \quad (2)$$

where $c_{k\sigma}^\dagger$ ($c_{k\sigma}$) are the creation (annihilation) operators for the conduction spin- $\frac{1}{2}$ fermionic bath with the energy dispersion $\epsilon_{k\sigma}$ and d_σ^\dagger (d_σ) for the impurity orbital with energy $\epsilon_{d\sigma}$, U is the on-site Coulomb interaction between the electrons on the impurity, and $V_{k\sigma}$ is the coupling between the bath and impurity orbital. The effective parameters ϵ_k and $V_{k\sigma}$ enter the hybridization function

$$\Delta_\sigma(i\omega_n) = \sum_k \frac{|V_{k\sigma}|^2}{i\omega_n - \epsilon_{k\sigma}}, \quad (3)$$

which is found by solving a self-consistent condition. Here $\omega_n = (2n+1)\pi T$ is the Matsubara frequency for fermions with n being integer and T the temperature. The impurity Green's function maps onto the site-diagonal Green's function of the original lattice Hamiltonian by the relationship:

$$G_{d\sigma}(i\omega_n) \equiv G_{ii\sigma}(i\omega_n) = \int_{-\infty}^{\infty} \frac{\rho_\sigma^{(B)}(\varepsilon) d\varepsilon}{i\omega_n - (\varepsilon - \mu) - \Sigma_\sigma(i\omega_n)}, \quad (4)$$

where $G_{d\sigma}(i\omega_n)$ is the Fourier transform of the impurity Green's function $G_{d\sigma}(\tau - \tau') = -\langle T_\tau [d_\sigma(\tau) d_\sigma^\dagger(\tau')] \rangle$ determined from the impurity Hamiltonian Eq. (2) while $G_{ii\sigma}(i\omega_n)$ is the site-diagonal Green's function corresponding to the lattice Hamiltonian in Eq. (1), $\rho_\sigma^{(B)}(\varepsilon)$ is the Bloch density of states (the $U = 0$ density of states of Eq. (1)) and μ is the chemical potential. This procedure indicates that Δ_σ in the present context, in contrast to the original SIAM model [4], is not known *a priori*. For infinite dimensional lattices or the Bethe lattice with infinite coordination number as we are considering here,

the self-energy is site-diagonal and the DMFT becomes exact. In addition, for $z \rightarrow \infty$, the non-interacting Bloch density of states is semielliptic, which reduces the self-consistency condition to:

$$\Delta_\sigma(i\omega_n) = t^2 G_{d\sigma}(i\omega_n), \quad (5)$$

with $\epsilon_{d\sigma} = -\mu$ for the paramagnetic case. Keeping the hybridization function spin dependent allows the approach to also be applied to the ferromagnetic ordering case.

If one is able to solve the SIAM for arbitrary parameters (i.e., $\epsilon_{k\sigma}$ and $V_{k\sigma}$ via Δ_σ), the lattice model can be solved through self-consistent iteration, by using the following procedure: First, given a hybridization function, one solves the SIAM for the impurity Green's function (or self-energy); Second, through the self-consistency condition, Eq. (5), a new hybridization function is obtained. The procedure is then iterated until the self-consistency is achieved.

The EOM approach corresponds to a resummation of low-order hopping process, but requires a decoupling

scheme. We have used the one introduced by Appelbaum and Penn [15] and Lacroix [16] (APL), which is known to capture the right qualitative feature of physics at low temperatures. Briefly, the EOM method consists of differentiating the Green's function $G_{d\sigma}(\tau - \tau')$ with respect to the imaginary time τ , thereby generating higher-order Green's functions which must be approximated in order to close the equations for $G_{d\sigma}(\tau - \tau')$. Since the time derivative of a Heisenberg operator is determined by its commutator with the Hamiltonian, it follows:

$$\left(-\frac{\partial}{\partial \tau} - \epsilon_{d\sigma}\right) G_{d\sigma}(\tau - \tau') = \delta(\tau - \tau') + U G_{d\bar{\sigma}\sigma}(\tau - \tau') + \sum_k V_{k\sigma}^* G_{k\sigma}(\tau - \tau'). \quad (6)$$

On the right-hand side of Eq. (6), there are two new Green's functions: $G_{k\sigma}(\tau - \tau') = -\langle T_\tau [c_{k\sigma}(\tau) d_\sigma^\dagger(\tau')] \rangle$, and the two-particle Green's function $G_{d\bar{\sigma}\sigma} = -\langle T_\tau [n_{d\bar{\sigma}}(\tau) d_\sigma(\tau) d_\sigma^\dagger(\tau')] \rangle$. By using the APL decoupling scheme to truncate this EOM one obtains:

$$G_{d\sigma}(i\omega_n) = \frac{1 - \langle n_{d\bar{\sigma}} \rangle}{i\omega_n - \epsilon_{d\sigma} - \Delta_\sigma + \frac{U \Sigma_{1\sigma}}{i\omega_n - \epsilon_{d\sigma} - U - \Delta_\sigma - \Sigma_{3\sigma}}} + \frac{\langle n_{d\bar{\sigma}} \rangle}{i\omega_n - \epsilon_{d\sigma} - \Delta_\sigma - U - \frac{U \Sigma_{2\sigma}}{i\omega_n - \epsilon_{d\sigma} - \Delta_\sigma - \Sigma_{3\sigma}}}, \quad (7)$$

where the occupancy probability is

$$\langle n_{d\sigma} \rangle = \int d\epsilon f_{FD}(\epsilon) \rho_\sigma(\epsilon), \quad (8)$$

with the spectral density $\rho_\sigma(\epsilon) = -\text{Im}[G_{d\sigma}(\epsilon + i\eta)]/\pi$

(η is an infinitesimal). The hybridization function Δ_σ represents the hopping of the electron with spin projection σ onto or out of the impurity site, while the other self-energies are due to the hopping of the electron with opposite spin projection $\bar{\sigma}$,

$$\Sigma_{i\sigma}(i\omega_n) = \sum_k A_{k\bar{\sigma}}^{(i)} |V_{k\bar{\sigma}}|^2 \left[\frac{1}{i\omega_n - \epsilon_{d\sigma} + \epsilon_{d\bar{\sigma}} - \epsilon_{k\bar{\sigma}}} + \frac{1}{i\omega_n - \epsilon_{d\sigma} - \epsilon_{d\bar{\sigma}} - U + \epsilon_{k\bar{\sigma}}} \right], \quad i = 1, 2, 3, \quad (9)$$

where $A_{k\bar{\sigma}}^{(1)} = f_{FD}(\epsilon_{k\bar{\sigma}})$, $A_{k\bar{\sigma}}^{(2)} = 1 - f_{FD}(\epsilon_{k\bar{\sigma}})$, $A_{k\bar{\sigma}}^{(3)} = 1$ with the Fermi distribution function $f_{FD}(\epsilon) = [1 + \exp(\epsilon/T)]^{-1}$. By performing an analytic continuation, i.e., replacing $i\omega_n$ with $\omega + i\eta$, one arrives at the retarded Green's function, which is exactly identical to that derived directly from the real time approach [15, 16, 17]. The impurity Green's function $G_{d\sigma}$, as given by Eq. (7), is exact both in the non-interacting limit ($U = 0$) and in the atomic limit ($V_{k\sigma} = 0$). Since the accuracy of the EOM method depends on how good the decoupling scheme is, this is an important confirmation on the qual-

ity of the APL decoupling. It is also useful to note that at low temperatures, the EOM solution based on the APL decoupling scheme has the expected Kondo resonance at the Fermi energy [18], originating from the self-energy, $\Sigma_{1\sigma}$, which is due to the virtual intermediate process where the impurity orbital is occupied by an electron of opposite spin $\bar{\sigma}$.

Physical quantities like the spectral function require a knowledge of the Green's function on the real frequency axis. For IPT, direct calculations of the self-energy on the real frequency axis are very complicated because of

multiple-dimension integrals. Instead one first performs the calculation on the imaginary frequency axis and then computes the spectral function by performing an analytic continuation by a Pade approximation. For this kind of treatment to be successful the quantities involved in the Green's functions and the self-energies need to be expressed in terms of the hybridization function as a whole. In the current approach, the three self-energies in Eq. (9)

cannot be represented as functions of Δ_σ . However, by introducing a line-width function

$$\Gamma_\sigma(\omega) = -\frac{1}{\pi} \text{Im}[\Delta_\sigma(\omega + i\eta)], \quad (10)$$

one can instead rewrite Eq. (9) as:

$$\Sigma_{i\sigma}(i\omega_n) = \int d\epsilon A^{(i)}(\epsilon) \Gamma_{\bar{\sigma}}(\epsilon) \left[\frac{1}{i\omega_n - \epsilon_{d\sigma} + \epsilon_{d\bar{\sigma}} - \epsilon} - \frac{1}{-i\omega_n + \epsilon_{d\sigma} + \epsilon_{d\bar{\sigma}} + U - \epsilon} \right], \quad i = 1, 2, 3. \quad (11)$$

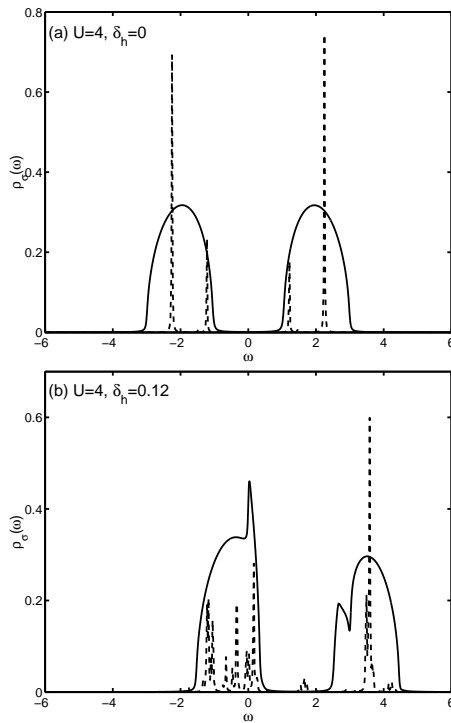


FIG. 1: The spectral density as a function of energy for $U = 4$ and the hole doping $\delta_h = 0$ (a) and 0.12 (b). Thick solid line: EOM approach. Thin dashed line: ED (6 sites). For clarity, the intensity from the ED is scaled down by a factor of 16 (a) and 8 (b). The parameter $\eta = 0.01$. $\omega = 0$ corresponds to the Fermi energy.

In order to work on the imaginary frequency axis, at each iteration step a Pade approximation for Γ_σ would be required, which would introduce significant numerical errors and make the convergence difficult. Since the occupancy probability given by Eq. (8) and the self-energies given by Eq. (11) all involve only one-dimensional integrals, we find it is more efficient to implement the technique directly on the real-frequency axis. For this purpose, we divide the relevant energy range into segments and use the Simpson's rule in combination with

the Neville's polynomial interpolation algorithm to do these integrals [19]. In the actual calculation, we use two iteration loops: The inner loop is for the occupancy probability $\langle n_{d\sigma} \rangle$ for a fixed line-width function Γ_σ . After the convergence of the inner loop is achieved, Γ_σ is updated through Eqs. (5) and (10) in the outer loop. We find the algorithm is very efficient: in most cases a solution is found within 20 iterations. It is also remarkable that the algorithm provides stable convergence with respect to different guesses for the initial hybridization function used to start the calculation.

In the following discussions, all energies are measured in units of the half bandwidth $D = 2t = 1$. We take the temperature $T = 0.01$. In Fig. 1, we show the spectral density, $\rho_\sigma(\omega)$, as a function of energy for $U = 4$ and for values of the hole doping $\delta_h (= 1 - \sum_\sigma \langle n_{d\sigma} \rangle)$ of 0 and 0.12. As shown in Fig. 1(a), in the undoped case (i.e., half filling), the spectral density displays only the lower and upper Hubbard bands separated by a Mott insulator gap. Due to the particle-hole symmetry, these two bands are symmetric to each other around the Fermi energy. At finite doping (e.g., $\delta = 0.12$ as shown in Fig. 1(b)), the spectral density exhibits a sharp quasiparticle resonance peak at the Fermi energy, and two broad satellite features corresponding to the lower and upper Hubbard bands, as would be expected for a doped Mott insulator. Since the particle-hole symmetry is broken upon doping, the spectral density is no longer symmetric with respect to the Fermi energy. To demonstrate the accuracy of the present approach, we have also run the ED algorithm developed by Caffarel and Krauth [12] for 6 sites with the same parameter values. The output is shown by thin dashed lines in Fig. 1. As one can see, the results obtained from the EOM approach compare well with those from the exact diagonalization method. Like IPT, in addition to computational efficiency, the advantage of the EOM approach is that it can give a very smooth shape for the spectral density. The ED method can at best give a correct overall spectral density distribution with sharp

spike-like structures due to the small number of orbitals being used. Because the use of a large number of orbitals in the ED method would exceed current computational capabilities, we conclude that the EOM approach may be a useful alternative.

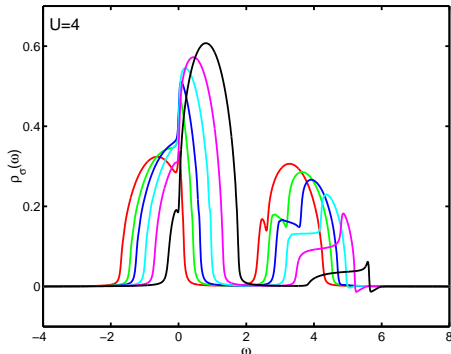


FIG. 2: (Color) The evolution of the spectral density with increasing hole doping $\delta_h = 0.06, 0.16, 0.26, 0.44, 0.64, 0.88$ (counted from the left). The parameter $\eta = 0.02$.

With increased confidence due to our success in calculating the spectral function, we now turn to the evolution of the spectral density with hole doping. These results are shown in Fig. 2. The most striking features are as follows: When the chemical potential crosses the edge of the lower Hubbard band (i.e., when hole doping begins), a Kondo resonance peak shows up at the Fermi energy. At the same time, an anti-resonance dip occurs in the upper band. As the doping increases, there continues to be a peak-like feature near the Fermi energy that gradually decreases in intensity. The effects on the upper Hubbard band are even more dramatic, as the anti-resonance dip evolves into a feature that shifts more deeply into the upper Hubbard band and eventually becomes more of a plateau, with the spectral weight continuing to be transferred out of the upper Hubbard band. The hole doping dependence of the spectral weight reflects the different parameter regimes of the SIAM. Within the EOM approach, one does not find a narrowing of the upper Hubbard band. This picture of the spectral density evolution is different from that based on the iterative perturbation theory. Since the two approaches are so different, we find it very difficult to draw a judgement on which picture is more reasonable without a large-size ED calculation to check the results. We have also studied the electron doping case, and found a similar spectral weight transfer (now out of the lower Hubbard band).

To summarize, we have proposed an EOM approach as an impurity solver for dynamical mean field theory. The solution for the impurity Green's function is exact in the non-interacting and isolated-site limits. The technique has been implemented directly on the real-frequency axis, which turns out to be computationally efficient. As an illustration, we have studied a finite- U Hubbard model

defined on the Bethe lattice with infinite connectivity at arbitrary filling. Depending on the filling, all typical features of strongly correlated materials such as the quasiparticle peak at the Fermi energy, and lower and upper Hubbard bands, have been produced for the spectral density. The main results have also been compared with exact diagonalization and found in good agreement. In addition, a new picture of the spectral density evolution as a function of filling factor is found, which should be tested by future exact diagonalization studies with a large number of orbitals. The extension of this approach to the multi-orbital case constitutes a future investigation, which will be very useful for *ab initio* DMFT applications to real materials.

Note Added: In the final stage of this work, we became aware of a preprint by H. O. Jeschke and G. Kotliar [20], where a similar approach was proposed. Their study focused on the case of an infinite Hubbard interaction such that the technique could be directly implemented in Matsubara frequency. In that case, only the quasiparticle peak and lower Hubbard band are the relevant characteristics. It is encouraging to see that in the comparable region, both of our studies show a very similar shape for the spectral density.

Acknowledgments: One of us (JXZ) is grateful to Q. Si for helpful discussions. This research is supported by the Department of Energy under contract W-7405-ENG-36.

-
- [1] For a review see A. Georges *et al.*, Rev. Mod. Phys. **68**, 13 (1996).
 - [2] For the extension of the DMFT see, Q. Si and J. L. Smith, Phys. Rev. Lett. **77**, 3391 (1996); J. L. Smith and Q. Si, Phys. Rev. B **61**, 5184 (2000); R. Chitra and G. Kotliar, Phys. Rev. Lett. **84**, 3678 (2000); O. Parcollet, G. Biroli, and G. Kotliar, Phys. Rev. Lett. **92**, 226402 (2004) and references therein.
 - [3] For the initial success of *ab initio* DMFT see S. Y. Savrasov, G. Kotliar, and E. Abrahams, Nature **410**, 793 (2001).
 - [4] P. W. Anderson, Phys. Rev. **124**, 41 (1961).
 - [5] M. Jarrell, Phys. Rev. Lett. **69**, 168 (1992).
 - [6] M. Rozenberg, X. Y. Zhang, and G. Kotliar, Phys. Rev. Lett. **69**, 1236 (1992).
 - [7] A. Georges and W. Krauth, Phys. Rev. Lett. **69**, 1240 (1992).
 - [8] A. Georges and G. Kotliar, Phys. Rev. B **45**, 6479 (1992).
 - [9] X. Y. Zhang, M. J. Rozenberg, and G. Kotliar, Phys. Rev. Lett. **70**, 1666 (1993).
 - [10] H. Kajueter and G. Kotliar, Phys. Rev. Lett. **77**, 131 (1996).
 - [11] M. Potthoff, T. Wegner, and W. Nolting, Phys. Rev. B **55**, 16132 (1997).
 - [12] M. Caffarel and W. Krauth, Phys. Rev. Lett. **72**, 1545 (1994).
 - [13] Q. Si *et al.*, Phys. Rev. Lett. **72**, 2761 (1994).

- [14] J.-X. Zhu, D. R. Grempel, and Q. Si, Phys. Rev. Lett. **91**, 156404 (2003).
- [15] J. A. Appelbaum and D. R. Penn, Phys. Rev. **188**, 874 (1969).
- [16] C. Lacroix, J. Phys. F **11**, 2389 (1981).
- [17] Y. Meir, N. S. Wingreen, and P. A. Lee, Phys. Rev. Lett. **66**, 3048 (1991).
- [18] T. K. Ng and P. A. Lee, Phys. Rev. Lett. **61**, 1768 (1988); Y. Meir, N. S. Wingreen, and P. A. Lee, Phys. Rev. Lett. **70**, 2601 (1993).
- [19] W. H. Press *et al.*, *Numerical Recipes in Fortran* (Cambridge University Press, Cambridge, 1992).
- [20] H. O. Jeschke and G. Kotliar, cond-mat/0406472.